

UNCLASSIFIED

AD 4 4 5 1 0 1

DEFENSE DOCUMENTATION CENTER

FOR

SCIENTIFIC AND TECHNICAL INFORMATION

CAMERON STATION, ALEXANDRIA, VIRGINIA



UNCLASSIFIED

NOTICE: When government or other drawings, specifications or other data are used for any purpose other than in connection with a definitely related government procurement operation, the U. S. Government thereby incurs no responsibility, nor any obligation whatsoever; and the fact that the Government may have formulated, furnished, or in any way supplied the said drawings, specifications, or other data is not to be regarded by implication or otherwise as in any manner licensing the holder or any other person or corporation, or conveying any rights or permission to manufacture, use or sell any patented invention that may in any way be related thereto.

445101

CATALOGED BY DDC

AS AD NO.

OFFICE OF NAVAL RESEARCH

Contract Nonr-1866(36)

TECHNICAL REPORT

THE MECHANISM OF THE ACETYLENE-OXYGEN REACTION
IN SHOCK WAVES

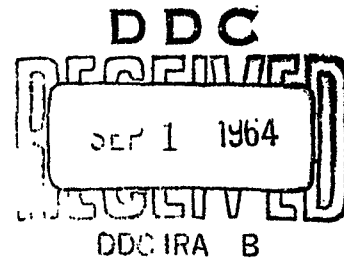
G. P. Glass, G. B. Kistiakowsky,
J. V. Michael, and H. Niki

Submitted to
JOURNAL OF CHEMICAL PHYSICS

Department of Chemistry
Harvard University
Cambridge, Massachusetts 02138

August, 1964

Reproduction in whole or in part is permitted for any purpose
of the United States Government.



Contribution from the Gibbs Chemical Laboratory

Harvard University

Cambridge, Massachusetts

THE MECHANISM OF THE ACETYLENE-OXYGEN

REACTION IN SHOCK WAVES

G. P. Glass, G. B. Kistiakowsky,

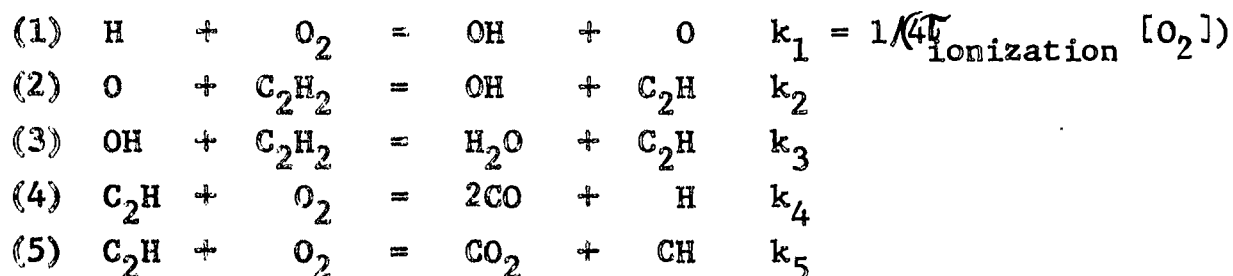
J. V. Michael, and H. Niki

ABSTRACT

The oxidation of acetylene has been studied using sufficiently high gas densities and concentrations of inert gas to keep the reaction isothermal and reduce boundary layer effects. The induction periods and exponential time constants of the oxidation have been measured using the observations of: (a) chemiluminescence and gas conductivity in incident and in reflected shock waves, and (b) total ionization and product formation using a time-of-flight mass spectrometer in reflected shock waves. The results are internally consistent, and the time constants τ are best represented by the following equation:

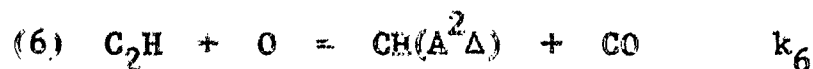
$$\log_{10}(\tau[\text{O}_2]) = -14.29 + 17,000/4.58 T$$

in units of sec. moles/cm³. Induction periods are about 8 times longer. The following reaction mechanism is most consistent with the data:



Reaction (1) is rate controlling, the above defined value of k_1 agreeing well with the work of others. The time constants τ for CO, CO₂, and H₂O are identical indicating that they are all formed in the branching chain reaction, but those of ionization and luminescence are half as large. Diacetylene formation is observed in acetylene rich mixtures. Experiments with added CO indicate that reaction (5) is initially the main source of CO₂.

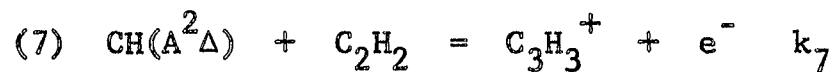
The reaction:



explains the observed chemiluminescence well.

ABSTRACT (Page 2)

Experiments with the mass spectrometer show that $C_3H_3^+$ is the first ion observed. Other experiments suggest that the simple reaction:



is not responsible for the ionization. Other possible mechanisms for the formation of $C_3H_3^+$ are discussed.

THE MECHANISM OF THE ACETYLENE-OXYGEN REACTION IN SHOCK WAVES

Introduction

The oxidation of acetylene by oxygen in flames has been extensively studied in several laboratories^{1,2,3} and valuable

-
1. C.P. Fenimore and G.W. Jones, J. Chem. Phys., 39, 1514 (1963).
 2. K.H. Homann, M. Mochizuki and H.Gg. Wagner, Z. phys. Chem. N.F. 37, 299 (1963).
 3. R.M. Fristrom, W.H. Avery and C. Grunfelder, Symp. Combust. 7th, London and Oxford Univ., 1958, 304 (1959).
-

information has been obtained about the reaction kinetics. These flames exhibit intense chemi-ionization which has been studied by mass spectrometric and other techniques.^{4,5,6,7}

-
4. J.A. Green and T.M. Sugden, Symp. Combust. 9th, Cornell Univ., 1962, 607 (1963).
 5. H.F. Calcote, Symp. Combust. 9th, Cornell Univ., 1962, 622 (1963).
 6. E.M. Bulewicz and P.J. Padley, Symp. Combust. 9th, Cornell Univ., 1962, 638 (1963).
 7. S. De Jaegere, J. Deckers and A. Van Tiggelen, Symp. Combust. 8th, California Institute of Technology, 1960, 155 (1962).
-

The species, HCO^+ , has been repeatedly suggested to be the primarily formed ion and a mechanism for its formation has been discussed;^{4,5,6,7,8} its observed concentration is low compared

-
8. C.W. Hand and G.B. Kistiakowsky, J. Chem. Phys., 37, 1239 (1962).
-

to other ions. The chemi-luminescence in acetylene-oxygen flames is due to a variety of emitters, the $\text{CH}(\text{A}^2\Delta \rightarrow \text{X}^2\Pi)$ system, the C_2 Swan bands, the fourth positive system of CO, and the HCO Vaidya flame bands having been observed.⁹

-
9. A.G. Gaydon, The Spectroscopy of Flames (Chapman and Hall Ltd., London, 1957), p. 113.
-

The oxidation has also been studied in shock waves in which the reactants were highly diluted by inert gas so that the reaction proceeded under nearly isothermal conditions which are determined by the parameters of the shock wave. Measurements of the far ultraviolet ($\text{CO}; A^1\Pi \rightarrow X^1\Sigma$)¹⁰ and visible (CH and C_2)

-
10. G.B. Kistiakowsky and L. Willard Richards, J. Chem. Phys., 36, 1707 (1962).
-

radiation, and of ionization,⁸ established exponential growth of these phenomena, indicative of a branching chain reaction. Measurements of the induction period, t_i , arbitrarily defined as the time elapsed before a specific level of signal is observed, and also of the exponential time constant, τ , led to the identification of the branching reaction, $\text{H} + \text{O}_2 = \text{OH} + \text{O}$, as the rate determining step. Studies with a high speed mass spectrometer assisted in the development of the probable reaction mechanism.¹¹

11. J.N. Bradley and G.B. Kistiakowsky, J. Chem. Phys., 35, 264 (1961).
-

More recently, using an improved apparatus, the proposed mechanism has been modified¹² and the ion, C_3H_3^+ , has been identified as

12. J.E. Dove and D.M. Moulton (To be Published in Proc. Roy. Soc.)
-

the probable primary ion.¹³ This ion had been observed in flames

13. G.B. Kistiakowsky and J.V. Michael, J. Chem. Phys., 40, 1447 (1964).
-

by others but was considered to be of secondary importance.

The present paper reports the results of further studies with shock waves.

Experimental

Earlier work from this laboratory on chemi-luminescence and chemi-ionization with a Langmuir probe was troubled by shock imperfections due to the low gas densities employed, and the resulting uncertainties in temperatures led to scattered experimental points and frequently to useless data. The shock wave experiments here described were made, therefore, on gases at 5 Torr or higher initial pressures. Preliminary experiments indicated that the total visible chemi-luminescence has a more complex time dependence than that of CH^* and, therefore, an interference filter (Baird Atomic, Type B1, peak at 4330 \AA with 47% transmission, peak half width of 60 \AA) was used in front of an RCA 1P28 photomultiplier to isolate the main band of the $\text{A}^2\Delta \rightarrow \text{X}^2\Pi$ transition of CH. Because of concern about the effects of gas flow in the incident shock wave on the output of a Langmuir probe, a movable flat back plate could be located 7 millimeters behind the plane containing the probe and the optical slits so that experiments could also be made on the stationary gas behind the reflected wave. Finally, in experiments on the quantitative relation between the CH^* chemi-luminescence and the chemi-ionization, the signals from the two detectors were fed into the two input channels of a Type CA Tektronix preamplifier which was operated in the "chopped" mode. In this mode the signals from each input are displayed alternately, with each input display being shown for 5 microseconds. Thus the temporal relationship of the two signals could be accurately established.

The Langmuir probe was used both at a positive and negative potential of 5 volts. The former gives approximately 10^2 higher output because some of the negative charge is carried by the more mobile free electrons. However, flame work has shown

that some charge is also carried by negative ions. This circumstance makes quantitative readings of negative probe current less meaningful because the gas conductivity is strongly dependent upon the extent of electron-molecule attachment reactions. For the more quantitative experiments the probe was used, therefore, at the negative potential.

The new shock tube - Bendix Time-of-Flight (TOF) mass spectrometer was the other apparatus used and this has been recently described.¹² Further improvements in the electronics of the spectrometer have led to the resolution of the chemi-ion mass spectrum and a reduction of the random noise in the spectra.

The ionizing electron beam duration was lengthened from 0.25 to 1.5 $\mu\text{sec.}$ per cycle, thus significantly increasing the ion yields from neutral species without much loss in resolution. A +7 volt d. c. potential was applied to the ion focus grid and the -200 volt ion focus pulse was shortened from 2.5 to 1.5 $\mu\text{sec.}$ and its decay time was decreased from 10 to less than 3 $\mu\text{sec.}$ The ion lens in the drift tube of the mass spectrometer was turned on, thus increasing the collection efficiency at the multiplier.

The mass resolution of the chemi-ions can be explained on the basis that chemi-ions (along with neutral molecules) emerge into the ionizing region of the mass spectrometer from the pinhole at thermal velocities and sense the +7 volt potential. Calculation shows that it takes about 1.4 $\mu\text{sec.}$ to stop, repel, and destroy an ion by discharging it at the grounded end plate of the shock tube. Consequently a sheath of ions is formed about 0.5 to 1.0 millimeters in front of the pinhole, and thus, an "ion sample" is stored until the negative ion focus pulse is applied to draw them out (as well as those formed by electron

impact when the electron beam is in use) forming a resolved spectrum. The random noise is due to chemi-ions entering the spectrometer during the application of the ion focus pulse.

Some experiments were made with an additional grid (trapping grid) placed between the end plate of the shock tube and the ion focus grid. The ion focus grid was held at +12 volts d. c. and was pulsed to -200 volts for 0.1 μ sec. per cycle, while the trapping grid, held at -6 volts d.c., was pulsed to +11 volts with a synchronized mirror image of the ion focus pulse. Highly resolved chemi-ion mass spectra with substantial decrease in noise were obtained by this method.

The spectrometer was operated at either 20 or 50 kilocycles. Up to seven consecutive mass spectra were displayed on each of five Tektronix 531 or 531A oscilloscopes triggered in sequence.¹²

Because of concern about the boundary layer effects in experiments with the TOF mass spectrometer, most of the present experiments were performed not with a pinhole in a thin end plate of the shock tube but with a miniature divergent conical nozzle, 1 millimeter long and 1 millimeter base diameter with a 0.12 to 0.18 millimeter diameter pinhole at the apex. The cone was pressed into 0.010 inch stock copper sheet, and the pinholes were pierced with a sewing needle. According to semi-quantitative calculations¹² a reentrant nozzle of this height should greatly delay the effects of the boundary layer at the end plate.

Gas mixtures for the TOF apparatus were 5% reactants and 95% Kr or Ne unless otherwise specified. These inert gases were used because krypton ions have higher mass than any ions of primary interest, and neon has such a small ionization cross section for 34 volt electrons that mass 20 and 22 ions do not

swamp the multiplier. Neon 20 and 22 peaks were also used as an internal calibration of shock wave conditions. Gas mixtures for the apparatus using a Langmuir probe and photocell were normally one part of reactants to ninety-nine parts argon.

The gas mixtures were made from highly purified rare gases obtained from AIRCO. Acetylene was obtained from Matheson Company and was purified by taking either middle or top fractions of a bulb to bulb distillation. Oxygen was prepared from potassium permanganate decomposition or obtained from AIRCO. $O^{18}O^{18}$ obtained from Yeda Research & Development Company was used in a few experiments and was of 98.4% isotopic purity. Gas mixtures were stirred for at least 24 hours before use.

Shock parameters were calculated from ideal shock relations. Incident and reflected wave calculations were made with the aid of an IBM 1620 computer.

EXPERIMENTAL RESULTS

I. Effects of Shock Wave Imperfections.

In earlier papers from this laboratory the quantitative meaning of some experiments was in doubt due to wave imperfections. Table 1 shows that with the now improved procedures the values of exponential time constants obtained from measurements of chemiluminescence and total ionization in incident and reflected waves are quite consistent.

The data already published¹² with the new TOF spectrometer apparatus suggested significant effects due presumably to the growing boundary layer around the shorter nozzle used. The definition of induction period was based on the formation of CO and H₂O. In the following the induction period is defined

as the time elapsed before observation of an arbitrarily chosen low level of total ionization signal. Since chemi-ionization is the more sensitive indicator, the induction periods observed in the present work are slightly shorter than in the former. This difference in definition explains why the measurements already published with the new TOF apparatus disagreed with earlier work and suggests that boundary layer growth was not as significant as was implied.

So that chemi-ionization could be used as the indicator of reaction, the pulsing circuitry of the TOF was turned off and a steady negative potential of 22 volts was applied to the ion focus grid. Then a substantial fraction of all chemi-ions entering the spectrometer reaches the multiplier in a steady stream after a delay of 1-5 μ sec. The scope was triggered by a velocity gauge located 12.7 cm. from the end plate, and the start of the sweep was registered on the raster scope. The results were records of total ion current similar to that shown in the earlier publication¹² but on an expanded time scale since the sweep was chosen as 100 μ sec/cm. The accuracy of the measured induction periods when operating in this mode is comparable to that obtained with the Langmuir probe. However, the gas is sampled from a region much closer to the end plate of the shock tube with the TOF apparatus.

The results are shown in Table 2, and it is clear that induction periods measured by chemi-ionization in reflected waves with the TOF agree remarkably well with the earlier data obtained by Richards¹⁰ from measurements of chemiluminescence in incident shocks. Moreover, the data of five new runs with the Langmuir probe in incident waves agree quite well with the rest. The last set of data in Table 2 refers to mixtures rich in acetylene. Apparently in these runs at temperatures greater than 1800°K

either the initiation processes are greatly accelerated or the rate controlling reaction in the branched chain mechanism changes. The former is probably the case since the observed overall rate of reaction at a given temperature in this mixture is approximately the same as in stoichiometric mixtures containing the same oxygen concentration at the same temperature. It might be added that standard deviations from a least squares line can be substantially reduced in Table 2 by choosing $\text{Log } (t_i[\text{O}_2]^{\frac{1}{2}})$ instead of $\text{Log } (t_i[\text{O}_2])$ versus $1/T$, but the effect of acetylene concentration on the induction periods (and exponential time constants) is statistically insignificant except in the case already mentioned above.

The comparison of the least squares line fitting the data of Table 2 with that obtained earlier from chemiluminescence measurements in incident waves^{8,10} shows that these TOF measurements are not significantly affected by boundary layer effects.

Table 3 compares exponential time constants derived from the early rising portion of total ionization in reflected waves measured by the TOF with two other techniques in incident waves. The three sets of data agree extremely well, again substantiating the validity of the techniques employed.

It should be noted that the accuracy of the measurements of the induction period, t_i , is greater than that of the time constant, τ . The ratio, t_i/τ , is about 8, and both have experimentally an identical positive temperature coefficient given by $E = 17,000 \pm 500$ cal/mole.

In order to ascertain when boundary layer effects become important, as they eventually must, a few runs were made with the TOF equipped with (a) a shorter nozzle and (b) a pinhole in the flat end plate. Since the boundary layer grows from the end

plate into the reacting gases, substitution by either (a) or (b) would presumably increase the effects of boundary layer. However, the observed induction periods fell into the range of data shown in Table 2. Thus, the induction periods are correctly measured with the TOF even under these extreme conditions.

However, some of the gas flowing into the TOF through the nozzle may come from the colder layers near the ~~and~~ plate of the shock tube after longer periods of time. An apparent cessation of the reaction before acetylene and oxygen have been consumed is actually observed, as in Fig. 1, and this effect is especially noticeable after long induction periods at lower temperatures.

II. Formation of Uncharged Reaction Products.

The general pattern of results is illustrated by Fig. 1 in which the peak heights of the parent ions from the reactants and products (as well as that of one chemi-ion, $C_3H_3^+$) have been plotted for a good but not an exceptional run on a semi-log scale against time. One observes that as the concentrations of O_2 and C_2H_2 begin to decrease, those of the products increase. Carbon monoxide appears first in measurable quantities and its yield throughout the reaction is much higher than those of H_2O and CO_2 . By the time the latter are formed in measurable quantities the recorded spectra become less accurate due to the increase in the noise level produced by random chemi-ions. This accounts for the larger scatter of small peak heights measured near the end of the run.

In addition to the masses shown in Fig. 1, $m/e = 50$ (diacetylene) was also observed but only in mixtures rich in acetylene. At higher temperatures molecular hydrogen is also formed in measurable and increasing quantities.

Possible sources of uncertainty in the quantitative interpretation of the data obtained with the TOF are: (1) The peak heights of individual species are subject to random fluctuations because of the finite number of ions reaching the detector in each pulse. Also, after some progress of reaction, peak height measurements are more uncertain due to the presence of random chemi-ion noise. (2) The number of chemi-ions entering the mass spectrometer is more sensitive to the size of the pinhole than are neutral species. Apparently collisional destruction of the chemi-ions on the walls of the nozzle occurs and is therefore greater with the smaller pinhole. (3) Charge transfer reactions between the rare gas diluent and reactants or products in the mass spectrometer are not completely excluded even though they are apparently not important. Thus the peak height ratio of C_2H_2 to O_2 (before reaction) is independent of diluent (Ne or Kr). Furthermore static simulation of the density conditions present in the spectrometer during observations in shock heated gases for both C_2H_2 and Kr, shows no increase in $m/e = 26$ (C_2H_2) relative to the value obtained when only C_2H_2 is present. Finally, crude calculations of gas density in the plane of ionization by the electron beam indicate that a rate constant of 10^{-7} cc/sec. is needed for appreciable charge transfer reaction to occur. A value of 10^{-11} cc/sec. for $Xe^+ + C_2H_2 = Xe + C_2H_2^+$ has been reported.¹⁴

14. P.S. Rudolph, S.C. Lind, and C.E. Melton, J. Chem. Phys. 36, 1031 (1962).

Notwithstanding these limitations it has been possible to obtain some quantitative data with the TOF. To assess them one should note that in the type of branching chain mechanism proposed earlier^{8,10,11,12} all reactions are first order in intermediates, and therefore, the instantaneous concentrations of all

intermediates and products should have identical time dependence. It is of the simple form, $\exp(t/\tau)$, so long as reactants are not depleted. Fig. 1 and other runs show that τ actually increases with the progress of the reaction as it should, but the changes are larger than can be accounted for by the theoretical relation:¹⁰

$$(a) \quad [\tau]^{-1} = 2k_1 [O_2]$$

Either boundary layer development or product inhibition are mainly responsible for this behavior.

The time dependence of τ and the finding that peak heights of CO_2 and H_2O reach measurable magnitudes only after significant depletion of reactants has occurred necessitated a comparison of the rates of formation of the three main products, CO , CO_2 , and H_2O , during the same time interval of each run. Table 4 shows peak heights of these products measured in five consecutive runs. In general, as Fig. 1 indicates, only a few successive spectra of both CO_2 and H_2O display roughly exponential growth. The individually measured τ 's for these products and for CO during this small time interval are inaccurate because of experimental scatter, and the absolute values are about 6 to 10 times longer than the initially measured rate of chain branching (see for example Table 3). Nevertheless if one assumes that the change of τ with time is the same for all products (this is indicated from Fig. 1 and eq. (a)) and is invariant over the small temperature range ($125^\circ K$) of the experiments in Table 4, then one can combine the data of the five runs to obtain average τ 's at a standard condition by the following procedure. Table 3 shows that time constants depend on temperature as $\exp(+17,000/RT)$ and are inversely proportional to oxygen concentration. Therefore, the 50 $\mu\text{sec.}$ time interval between consecutive spectra in Table 4 was multiplied by the factor,

$$(b) \quad \frac{[O_2]_0}{5.36 \times 10^{-5}} \exp\left(\frac{17,000}{R} \times \left(\frac{1}{1700} - \frac{1}{T}\right)\right)$$

where $[O_2]_0$ and T are the initial concentration and the temperature of a run. This in effect reduces all of the experiments to a single condition as far as time interval is concerned, namely,

$[O_2] = 5.36 \times 10^{-5}$ moles/l and $T = 1700^\circ K$. A constant time increment was added to all data of a run so that the midpoints in the time axis of all runs coincided. This procedure corrects the induction periods which are dependent on temperature (see Table 2) to a single value. Finally the peak heights of a component (eg. CO) were multiplied by a constant factor, so that the geometric means of peak heights in all runs were the same. This procedure was necessary since the absolute sensitivity of the spectrometer was subject to change from run to run. The result of these operations (termed the center of gravity method, C.G.M.) except for experimental errors would be to place the logarithms of all peak heights of a component plotted against time on a straight line if the concentrations grow exponentially with time and the time constants obey equations (a) and (b). The result looks quite similar to the data shown in Fig. 3, only the present range of peak heights is considerably shorter. To these reduced data a least squares calculation was applied and the results for the three products are shown as $\bar{\tau}_0$ C.G.M. in Table 4. The standard errors in these values are quite small, substantiating the assumptions made in the calculations. Since the range of peak height values for a given component is small, the data do not prove exponential time dependence, but it is indicated as a good approximation.

Table 5 gives an analogous calculation for $\bar{\tau}_0$ C.G.M. for diacetylene compared with that of CO. Not enough H_2 is observed in the reaction to make a similar comparison possible.

The ions O^+ , OH^+ , and C_2H^+ consistently appear in the spectra but the time variations of their peak heights suggest

that they are most likely due to fragmentation of the parent molecule ions present. Thus no direct evidence for the presence of these intermediates has been obtained. As Fig. 1 indicates, about two percent of the initial concentration of reactants is detectable but the presence of the fragment ions makes it impossible to detect intermediates at such low concentrations.

A connection between peak heights and relative concentrations of CO, H₂O, and CO₂ was established by shock heating a known mixture of these gases in 94 percent Ne to about 1100°K. This procedure gave a relative ratio of peak heights to concentrations as 1 : 0.94 : 0.74 for CO : CO₂ : H₂O. Using this calibration and the fact that the three products grow at the same rate so that peak height ratios could be averaged over many consecutive spectra (see Table 4 and Fig. 1), the relative concentrations of the products were found in stoichiometric mixtures to be: CO = 10.0, CO₂ = 2.7, and H₂O = 3.2. These relative concentrations were found to be independent of temperature from 1500 to 2200°K.

In order to investigate the mechanism of CO₂ formation, some shock experiments were made with CO added to stoichiometric mixtures of acetylene-oxygen-neon at various temperatures. A ratio of CO/C₂H₂ = 0.7 was chosen since these conditions prevail in the reaction (see Fig. 1) when CO₂ is normally first observed. The experiments showed that the first appearance of CO₂ was delayed relative to oxygen depletion by about as much as in the normal reaction; that it appeared at about the same time as water and that their peak height ratio was about one to one, as in normal experiments. Experiments with such mixtures were then made using O¹⁸O¹⁸ at temperatures greater than 1900°K. By the time the CO₂ was discernible the CO¹⁸ peak height was about three times that of the added CO¹⁶. Both CO¹⁸O¹⁸ and CO¹⁸O¹⁶ were formed and

their relative concentrations were roughly three to one.

The addition of CO to the reaction mixture had a remarkable effect on the chemi-ion, $C_3H_3^+$. Normally (see Fig. 2-A) at temperatures greater than $1900^\circ K$ this ion decays quite rapidly, but with added CO the ion decayed slowly, passed through a minimum, and built up again toward the end of the available observation time, whereas the neutral species in these runs did not show this trend at all. This behavior is not clearly understood and a further investigation is required.

III. Chemi-ionization and Luminescence.

Resolved spectra of chemi-ions show consistently that $C_3H_3^+$ ($m/e = 39$ or $m/e = 42$ when using C_2D_2) appears first, grows exponentially with time, and is gradually replaced by other ions, the most abundant being H_3O^+ . Fig. 2 shows semi-quantitatively the observed temperature and composition trends in the build-up and decay of $C_3H_3^+$ and H_3O^+ . These trends (except for the absolute magnitude of the peaks) are unaffected by the gas flow through the nozzle. Even a simple pinhole in a thin plate gives similar results.

A comparison of the reactions in stoichiometric mixtures (Fig. 1, Fig. 2-A, and Fig. 2-B) shows that $C_3H_3^+$ decays more rapidly at high temperatures, giving rise to larger concentrations of H_3O^+ . The experiments on which Fig. 2-C and Fig. 2-D are based, were carried out under nearly identical temperature and density conditions except that the compositions were changed as indicated. $C_3H_3^+$ decays more rapidly and H_3O^+ builds up to its largest concentration when O_2 is present in excess. When C_2H_2 is present in excess, $C_3H_3^+$ still decays but H_3O^+ is almost nonexistent. The overall yield of ions is greatest at higher temperatures and in the stoichiometric mixture.

The following additional masses, along with their probable molecular formulas, were identified in the chemi-ion spectrum: Hydrocarbon ions; 15 (CH_3^+), 27 (C_2H_3^+), 51 (C_4H_3^+), 63 (C_5H_3^+), ca. 75 (C_6H_3^+ (?)). Oxygen containing ions; 31 (CH_3O^+), 33 (HO_2^+ (37 with $\text{O}^{18}\text{O}^{18}$)), 37 (H_5O_2^+), 43 ($\text{C}_2\text{H}_3\text{O}^+$), 46 (CH_2O_2^+). Groups of ions were also observed in the mass regions, 88-96 and 102-110. In no experiments was HCO^+ observed. This ion spectrum is in general agreement with that observed in low pressure flames.¹⁵

15. H.F. Calcote, S.C. Kurzius, and W.J. Miller, Symp. Combust. 10th, Cambridge, 1964, (to be published).

All of these ions have a positive temperature dependence. Masses, 63 and 75 arise slightly before H_3O^+ and attain concentrations comparable to H_3O^+ , although they decay rapidly whereas H_3O^+ attains a nearly constant high concentration. The other ions have relatively small concentrations, and can only be observed to arise later than C_3H_3^+ .

Fig. 1 demonstrates the consistent experimental finding that CO and C_3H_3^+ appear almost simultaneously when the reactants are not yet depleted and grow exponentially with time. Table 6 shows the least squares exponential time constants for CO and C_3H_3^+ for a series of runs. The τ 's calculated by the least squares equation (i) of Table 3 are also shown. The time constants, τ_0 , reduced to a standard condition ($T = 1400^\circ\text{K}$ and $[\text{O}_2] = 4.82 \times 10^{-5}$ moles/l) by an equation similar to eq. (b), are also shown. τ_0 C.G.M., obtained by the method described in connection with Table 4, is presented at the bottom of the table.

To conserve space, the individual peak heights (obtained at 20 $\mu\text{sec.}$ intervals) are not shown in Table 6 but are displayed in Fig. 3 after C.G.M. reduction. A crude estimate indicates that the absolute yield of C_3H_3^+ is about 10^{-6} of that of carbon monoxide.

The number of consecutive spectra in each run which was used to obtain the τ 's in the data presented in Table 6 and Fig. 3 is seen to vary considerably. Measured peak heights were plotted on a semilog scale against time (for example, see Fig. 1) and only all the points constituting the initial linear portion were used. Points which were obviously in the region of curvature were excluded, and since only slight curvature is seen in Fig. 3, it is felt that this procedure is valid.

The τ calc. from total ionization (38.6 μ sec.) agrees remarkably well with the τ_0 C.G.M. obtained for $C_3H_3^+$. This indicates that the ions measured by total ionization methods are indeed $C_3H_3^+$. As Fig. 3 indicates, mass peak 39 rises exponentially over a factor of about 20, and a similarly large exponential rise was observed by total ionization in the TOF.

With the Langmuir probe collecting positive ions the observed range of exponential growth was somewhat larger (see Fig. 4), undoubtedly because this probe is more sensitive and detects ionization slightly sooner. However, in acetylene rich mixtures, the probe, when negative, showed small but finite conductivity soon after the passage of the shock. This initial conductivity, which persisted throughout the induction period made it difficult to ascertain whether the further growth of ion current was exponential in time.

On the other hand the chemi-luminescence of CH is initially exponential in time under all conditions tested. By varying the amplification of the detector, exponential growth was followed over three decades in a series of identical shocks. The accuracy of measurements with the Langmuir probe and photomultiplier is illustrated in Fig. 4.

Tables 1 and 3 conclusively show that the time constants of chemi-ionization and CH luminescence are identical. Table 7

shows measurements of the ratios of positive ion current and chemiluminescent intensity which were made over the exponential part of the curves before much depletion of the reactants had occurred. Both signals were displayed on one oscilloscope in order that they could be quantitatively compared. As can be seen the ratio of probe current to luminescence depends on temperature and composition. Relative to luminescence the ionization is greatest in ^{lean or} stoichiometric mixtures and increases with rising temperature.

In 2 to 1 acetylene-oxygen mixtures a striking effect was observed. At 1890°K the ionization was small initially but continued to rise long after the luminescence had disappeared. However, at 2280°K the maximum probe current and peak luminescence occurred almost concurrently. In leaner mixtures the peaks of chemiluminescence and ionization occurred sensibly simultaneously under a variety of conditions.

DISCUSSION

I. The Rate Determining Process.

The data on induction periods, t_i , and time constants, τ , of ionization and luminescence collected in Tables 1, 2, 3, and 6 are in excellent agreement with earlier work^{8,10} and within themselves. The temperature coefficient (except for that of the highly acetylene rich mixtures of Table 3) is the same with all the techniques and is consistent with an activation energy of 17,000 cal/mole., the uncertainty being certainly not more than 500 cal/mole.

The composition dependence of the induction period is somewhat less than first order in oxygen concentration. No great significance can, however, be attached to this observation because the induction period depends not only on the rate determining chain

steps but also on the thermal initiation rate which has not been identified.

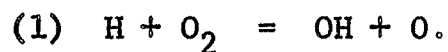
An analysis of the several sets of data of τ presented in the preceding section indicates that within experimental error the time constant is inversely proportional to oxygen concentration and is independent of acetylene concentration and the nature of the inert gas. A slight dependence on total gas concentration, making τ larger at higher concentrations, may be indicated by comparing present data with that obtained by earlier workers even though agreement is almost within the random scatter of the data.

The various methods used here give absolute (least squares average) values of τ which vary by a factor of 1.2 from the mean. The source of this variation is not clear since reflected waves with the apparatus using the Langmuir probe and photocell (Table 1) give larger τ 's than the TOF apparatus (Table 3) even though the sampling region is nearer to the end plate in the TOF experiments.

Within this minor uncertainty the present data may be considered to be free from gross error, and the most probable expression for the time constant using seconds and moles/cc as units is then given by:

$$(c) \quad \log_{10}(\tau [O_2]) = -14.29 + 17,000/4.58 T$$

The results of Table 6 clearly show that this τ is one half as large as that for CO formation. Therefore, eq. (a) suggests the relation^(d) $(\tau [O_2])^{-1} = 4 k_1$ for the chemi-ion $C_3H_3^+$ should hold where k_1 refers to:



Recently Westenberg and Fristrom¹⁶ summarized the results of

16. A.A. Westenberg and R.M. Fristrom, Symp. Combust. 10th, Cambridge, 1964, (to be published).

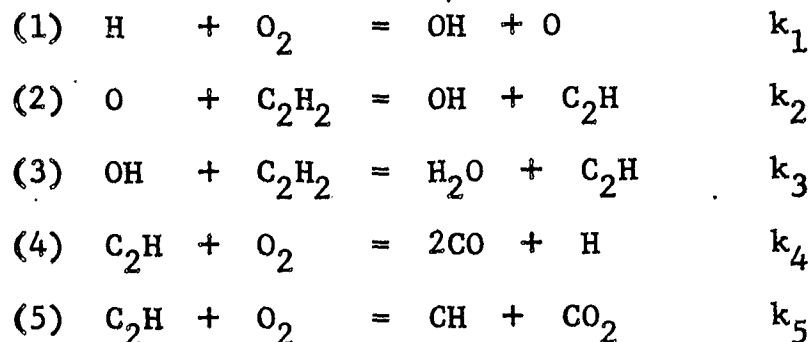
several investigations of the rate of reaction (1) as:

$$(e) \quad -\log_{10} (k_1) = -14.34 + 16,500/4.58 T.$$

This equation yields values of k_1 about four times larger than eq. (c) and (d). These workers note, however, that eq. (e) predicts rates of O_2 removal which are "several times" larger than actually observed and suggest that the real value of k_1 is 0.5 to 0.3 of that given by eq. (e).

The present results may, therefore, be regarded as a conclusive demonstration that reaction (1) is the rate determining step in the branching chain mechanism controlling the oxidation of acetylene in shock waves; they probably give a more accurate value of k_1 than eq. (e).

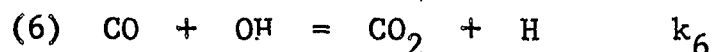
In the branching chain mechanism O atoms and OH radicals formed in reaction (1) regenerate H atoms. In the main, the mechanism previously proposed^{8,10,11,12} describes the observations best:



This mechanism ascribes the formation of H_2O and CO_2 to reactions (3) and (5) respectively, which are first order in intermediates, and therefore, require that the time constants

of their formation be identical to that of CO. This is indeed confirmed by the data in Table 4. Insofar as the standard deviations are concerned, these data are conclusive, but some doubts remain as to their validity since all τ 's in Table 4 are considerably larger than can be accounted for by the depletion of oxygen. The source of this discrepancy can only be surmised and has been discussed in the previous section.

In most experiments on flames the formation of CO₂ is ascribed to reaction (6).

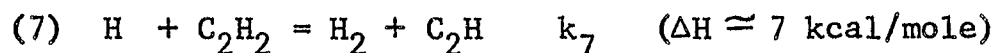


If this reaction were solely responsible for CO₂ formation, the time constant for CO₂ would be one half of that for CO since both CO and OH grow exponentially with time. Also, the ratio of CO₂ to H₂O yields should decrease markedly in acetylene rich mixtures since OH would have lower concentration due to the increased importance of reaction (3). Neither of these trends have been observed. In fact, the ratio of CO₂ to H₂O concentrations measured in several runs over the entire course of the reaction remains quite constant and is not grossly affected by composition changes, except late in the reaction in oxygen rich mixtures where CO₂ continues to grow after H₂O reaches a constant value. Hence it is concluded that CO₂ is formed in the early part of the reaction mainly by reaction (5). Reaction (6) may become important only when CO reaches a nearly constant value toward the end of the reaction.

These conclusions are supported by the observations that, when CO is added to the reaction mixture, both CO₂ and H₂O arise simultaneously and the CO₂ to H₂O ratio is unchanged from the system with no CO added. Since some CO¹⁸O¹⁶ is formed when CO is added to the reaction mixture containing O¹⁸O¹⁸, reaction (6)

may contribute especially at higher temperatures and in later stages of the reaction.

Reaction (2) is estimated to be rather endothermic ($\Delta H \approx 10$ kcal/mole), and therefore, k_2 cannot be very much larger than k_1 at the temperatures of these experiments. Thus, an effect of acetylene concentration on $\tilde{\tau}$ should have been observed in lean mixtures.¹⁰ Since no such effect was observed, either reaction (2) is faster than estimated or the O atoms must be able to react in other ways. One possible reaction sequence is:



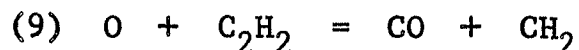
The sum of these reactions is reaction (2) and may be considered to be an alternate mechanism. Reaction (7) explains the formation of molecular hydrogen, especially at high temperatures since (7) must have an activation energy. The activation energy for (8) has been measured¹⁷ to be 9.2 kcal/mole. This indicates that (7) followed by (8) is probably a slower reaction pathway for O atoms than (2).

17. M.A.A. Clyne, Symp. Combust. 9th, Cornell Univ., 1962, 211 (1963).

The reaction mechanism proposed to this point (reactions (1) to (8)) requires a ratio of 3 for $([CO] + [CO_2])/([H_2O] + [H_2])$ if undetectable H atoms are still present in appreciable concentrations throughout the available observation time. Since the spectrometer was rather insensitive to molecular hydrogen, reliable values for the relative concentration of H_2 could not be obtained. However, it is interesting to note that $([CO] + [CO_2])/[H_2O]$ has an experimental value of 4.0 indicating that $[H_2]$ may be about 1.0

on the scale of $[CO] = 10.0$.

Another contributory process could be:

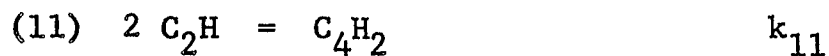


the subsequent fate of CH_2 being uncertain. Experiments in this laboratory on the room temperature reaction of O atoms and C_2H_2 suggest reaction (9) but indicate a rate too slow to be important in the branching chain mechanism. This reaction probably does occur, however, as a side reaction.

Due to the large standard errors present in the data of Table 5 some doubt still exists as to whether C_4H_2 is first or second order in intermediates. If it is first order as the data tend to suggest, then reaction (10) probably occurs.



This reaction has been proposed previously¹¹ and may be important in propagating the chain in acetylene rich mixtures. If it is second order then diacetylene is probably formed by reaction (11).

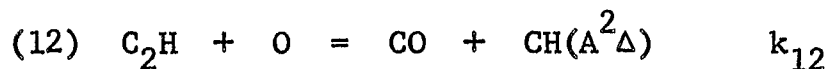


II. Chemi-ionization and Luminescence.

The mechanistic interpretation of chemi-ionization and luminescence must account for the consistent experimental findings that both phenomena: (i) grow exponentially with time in the initial stages of the reaction, (ii) have identical time constants which are half as large as that for CO (and probably for H_2O and CO_2) production, and (iii) have maximum yields in approximately stoichiometric mixtures.

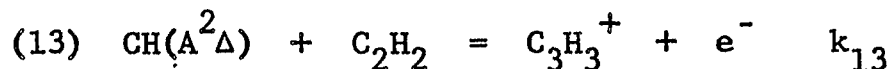
These facts suggest that both phenomena are intimately related to the branching chain mechanism and that they both are

produced by the reaction of two intermediates of the branching cycle. The most likely mechanism for the production of $\text{CH}(\text{A}^2\Delta)$ is:



Since, according to the proposed branching mechanism the concentration of C_2H must be reduced by reactions (4), (5), and (10) while that of O by reaction (2), the rate of reaction (12) must go through a maximum, as observed, when the $\text{O}_2/\text{C}_2\text{H}_2$ ratio is increased from lean to rich mixtures. Reaction (12) is estimated to be about 5 to 10 kcal/mole endothermic. This could account for the observed positive temperature coefficient of the CH luminescent yield and yet allow a sufficient rate of $\text{CH}(\text{A}^2\Delta)$ production to explain the absolute photon yield (10^{-4} photons/molecule C_2H_2 consumed).

Under all conditions investigated the ion, C_3H_3^+ , appeared first and at lower temperatures it was the only ion observed in large abundance. Furthermore, its concentration grows exponentially with time (Table 6 and Fig. 3). It has been suggested earlier¹³ that the reaction responsible for its production is:



Since this reaction would be competitive with $(\text{CH}(\text{A}^2\Delta \rightarrow \text{X}^2\Pi))$ photon emission, the ratio of ion ^{concentration} to the intensity of luminescence should be linearly dependent on acetylene concentration if the oxygen concentration is held constant. Table 7 demonstrates that this is definitely not the case. Also the experiments in acetylene rich mixtures in which luminescence was found to completely decay whilst ionization was still increasing, show that the connection between ionization and CH luminescence is not intimate.

Much effort has been devoted to developing the mechanism

for the formation of $C_3H_3^+$ but without much real success. Reaction (14) has been suggested by others^{4,5,6,7,8} as the primary



ion forming reaction and is a possibility since both CH and O atoms are chain intermediates of the proposed branching reaction. The heat of formation of CHO^+ is about 203 kcal/mole.¹⁸ For CHO^+

18. T. Mariner and W. Bleakney, Phys. Rev. 72, 792 (1947).

to remain undetected and to be manifested as $C_3H_3^+$ in the TOF it must react rapidly and directly with acetylene, forming $C_3H_3^+$ by reaction (15):

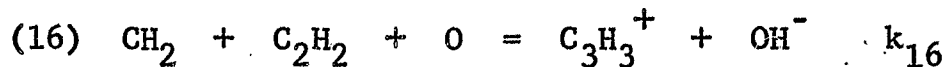


Reaction (15) implies a heat of formation for $C_3H_3^+$ of less than 210 kcal/mole, for CHO^+ not to be detected. The persistence of $C_3H_3^+$ at low temperatures also indicates that the $C_3H_3^+$ ion does not undergo fast ion-molecule reactions, suggesting again a low heat of formation. Thus, the $C_3H_3^+$ ion seen in these experiments cannot have a heat of formation of 270 kcal/mole. as proposed by Wiberg et al.¹⁹ The ion probably has a cyclic aromatic

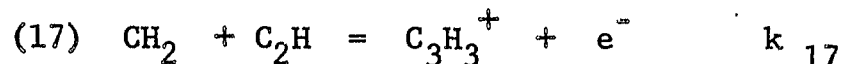
19. K.B. Wiberg, W.J. Bartley, and F.P. Lossing, J. Am. Chem. Soc., 84, 3980 (1962).

structure and derives stability from delocalization of its electron system as suggested in an earlier publication.¹³

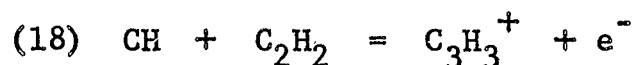
If reactions (14) followed by (15) actually occur, then CH must only be formed from reaction (5) since the results require that ionization be second order in intermediates. However, other more direct mechanisms can be written which satisfy this latter requirement. For example the over-all reaction:



is thermoneutral if the heat of formation of $C_3H_3^+$ is about 227 kcal/mole. The observation that some of the negative charge carriers are free electrons is probably not in conflict with reaction (16) because of high temperatures and comparatively low electron affinity of OH. Reaction (17) is thermoneutral if the heat of formation of $C_3H_3^+$ is 200 kcal/mole:



For reaction (18) to be thermoneutral the heat of formation of $C_3H_3^+$ must be ca. 195 kcal but $CH(X^2\pi)$ (ground state) would have to be formed by some process which is second order in intermediates and would rule out its formation by reaction (5):



The data of Table 7 require additional assumptions concerning the behavior of the intermediate reactants as a function of equivalence ratio with any of these mechanisms ((14) and (15), (16), (17), or (18)), unfortunately.

The rate of disappearance of $C_3H_3^+$ is dependent on temperature and mixture composition as shown in Fig. 3. This fact and the observation of higher hydrocarbon and oxygen containing ions suggest that $C_3H_3^+$ is not removed by ion-ion recombination reactions but rather undergoes oxidation and polymerization reactions both having activation energies.

Unfortunately a definitely preferred mechanism for the formation of $C_3H_3^+$ is still uncertain and we believe that a development of more powerful experimental techniques is required to solve this challenging problem.

ACKNOWLEDGEMENT

The authors wish to acknowledge the financial assistance of the National Science Foundation and the Office of Naval Research which made this research possible.

APPENDIX:

The heats of formation used in the thermochemical arguments in this paper are:

Species	$\Delta H_f(\text{kcal/mole})$
H	52
OH	9
O	59
C ₂ H	113
C ₂ H ₂	54
H ₂ O	-58
CO	-24
CH(² π)	142
CH ₂	85
CO ₂	-94
CH(A ² Δ)	208
HCO ⁺	203

FIGURE CAPTIONS

- Fig. 1. A semi-log plot of observed peak heights against time at 1526°K. Initial concentrations: $[C_2H_2] = 3.34 \times 10^{-5}$ mole/l; $[O_2] = 5.01 \times 10^{-5}$ mole/l; $[Ne] = 1.589 \times 10^{-3}$ mole/l. Note that H_2O and CO_2 peak height scales are altered as indicated to avoid confusion.
- Fig. 2. Smoothed plots of certain peak heights in four runs vs. time. Curves denote: (a) C_2H_2 ; (b) O_2 ; (c) $C_3H_3^+$; (d) CO ; (e) H_3O^+ . Experiments A and B are with $C_2H_2:O_2:Ne$ mixtures in a 2:3:95 ratio. Experiment C is with 2.5:2.5:95.0 ratio and experiment D is with 1.25:3.75:95.00 ratio.
- Fig. 3. A semi-log plot of C.G.M. reduced data of peak heights of $C_3H_3^+$ and CO versus time. See Table 6 for the τ 's of individual runs: \square and \blacksquare at 1206°K; ∇ and \blacktriangledown at 1370°K; \circ and \bullet at 1383°K; \circ and \bullet at 1410°K; \triangle and \blacktriangle at 1477°K; ϕ and \bullet at 1526°K.
- Fig. 4. A comparison of positive ion current and CH^* luminescence at 2150°K. $[C_2H_2] = 2.2 \times 10^{-5}$ mole/l; $[O_2] = 6.8 \times 10^{-5}$ mole/l; $[Ar] = 5.5 \times 10^{-3}$ mole/l. CRO signals are plotted on a semi-log scale against time.

TABLE 1

COMPARISON OF EXPONENTIAL TIME CONSTANTS τ IN
INCIDENT AND REFLECTED SHOCK WAVES

A. Reflected Shock Waves

$T(^{\circ}\text{K})$	$\frac{[\text{O}_2]}{\times 10^{+5}}$ moles/l	$\frac{[\text{C}_2\text{H}_2]}{\times 10^{+5}}$ moles/l	$\frac{[\text{Ar}]}{\times 10^{+3}}$ moles/l	$\tau_{(\mu\text{sec})}$ (Ionization)	$\tau_{(\mu\text{sec})}$ (CH Emission)	τ Calc. from least squares line
1815	10.8	2.7	7.2	6.9	6.9	7.0
1845	11.7	11.7	7.8	5.6	4.6	6.0
1845	10.8	10.8	7.2	7.6	6.1	6.5
1876	11.7	11.7	7.8	7.0	7.3	5.6
1890	11.7	5.8	7.8	5.7	6.1	5.6
1890	11.7	2.9	7.8	--	5.0	5.6
1890	13.4	4.3	8.0	5.0	5.6	4.9
1920	10.8	15.4	7.2	--	6.9	5.5
2020	10.2	2.5	6.8	5.4	4.6	6.7
2045	6.7	4.5	5.5	7.8	6.5	6.7
2081	10.2	10.2	6.8	3.5	4.0	4.0
2081	10.2	5.1	6.8	4.3	4.3	4.0
2180	6.7	2.2	5.5	4.8	4.6	5.2
2197	9.0	12.9	6.0	3.9	3.9	3.7
2238	9.0	9.0	6.0	3.5	3.5	3.6
2238	9.0	12.9	6.0	--	4.8	3.6
2281	9.0	4.5	6.0	3.5	3.3	3.3
2281	9.0	2.2	6.0	3.0	3.9	3.3

(i) Least squares fit to the data:

$$\log_{10}(\tau[\text{O}_2]) = -(11.17 \pm 0.03) + \frac{(17,100 \pm 3,800)}{4.58 T} \quad (\text{in sec. mole/liter units})$$

TABLE 1 (Page 2)

B. Incident Shock Waves

$T(^{\circ}\text{K})$	$\frac{[\text{O}_2]}{\times 10^{+5}}$ moles/l	$\frac{[\text{C}_2\text{H}_2]}{\times 10^{+5}}$ moles/l	$\frac{[\text{Ar}]}{\times 10^{+3}}$ moles/l	$\tau(\mu\text{sec})$ (Ionization)	$\tau(\mu\text{sec})$ (CH Emission)	τ Calc. from least squares line
1409	3.11	0.96	1.76	62.1	71.5	80.4
1409	3.11	0.96	1.76	64.1	64.1	80.4
1575	2.62	0.45	1.81	--	54.9	50.8
1596	3.22	0.99	1.81	--	36.6	37.9
1596	3.22	3.21	1.81	--	36.6	37.9
1615	3.22	0.99	1.81	52.2	--	36.6
1620	1.74	0.53	1.83	--	57.8	66.1
1625	3.22	0.99	1.81	36.6	33.8	35.1
1625	3.22	0.99	1.81	--	35.0	35.1
1650	3.22	3.21	1.81	--	35.2	32.3
1650	3.22	0.99	1.81	--	28.2	32.3
1763	1.77	0.54	1.86	39.9	44.9	41.8
1790	3.29	1.02	1.85	20.3	21.0	21.3
1800	3.29	1.02	1.85	18.9	18.9	20.7
1800	1.76	1.76	1.87	39.1	36.2	38.6
1810	1.77	0.54	1.86	--	40.6	37.9
1933	3.33	3.32	1.86	15.4	15.4	15.0
2115	1.85	0.57	1.94	20.1	19.4	18.4
2190	1.85	1.85	1.95	10.5	13.4	16.2

(ii) Least squares fit to the data:

$$\log_{10}(\tau[\text{O}_2]) = -(11.21 \pm 0.03) + \frac{(16,900 \pm 2,400)}{4.58 T} \quad (\text{in sec., mole/liter units})$$

TABLE 2

T(°K)	INDUCTION PERIODS			t_i (μsec)	$t_{i,calc.}$ (μsec)	Method
	[O ₂] x 10 ⁺⁵ moles/l	[C ₂ H ₂] x 10 ⁺⁵ moles/l	[M] x 10 ⁺³ moles/l			
1191	4.46	2.98	1.412	567	834	Total Ioniz., TOF, Reflected; in Ne.
1198	5.04	3.36	1.597	484	705	"
1272	8.91	5.94	2.818	436	231	"
1302	9.29	6.20	2.940	350	210	"
1308	4.72	3.19	1.491	448	413	"
1332	4.31	0.72	1.387	350	394	"
1344	4.90	3.27	1.552	396	331	"
1344	2.12	1.42	1.379	420	765	"
1379	4.41	0.74	1.419	304	313	"
1383	2.18	1.45	1.417	484	620	"
1391	2.12	1.42	1.379	391	608	"
1408	4.60	0.77	1.480	318	261	"
1409	9.67	6.45	3.059	189	124	"
1409	9.79	6.52	3.100	205	123	"
1431	4.89	3.26	1.547	194	224	"
1448	4.53	0.76	1.458	241	223	"
1473	5.06	3.38	1.602	208	184	"
1500	2.26	1.51	1.468	294	368	"
1539	5.21	3.48	1.649	131	139	"
1544	2.30	1.53	1.493	222	308	"
1558	10.42	6.95	3.680	86	65	"
1583	5.12	0.85	1.648	150	121	"
1627	5.31	3.54	1.680	120	101	"
1634	2.37	1.58	1.540	138	216	"
1692	2.39	1.59	1.552	147	179	"
1700	5.60	3.73	1.772	92	76	"
1729	5.70	3.80	1.803	82	68	"
1749	2.38	1.59	1.547	146	153	"
1764	5.73	3.82	1.815	69	61	"
1771	5.64	3.76	1.785	68	60	"

TABLE 2 (Page 2)

INDUCTION PERIODS						
$T(^{\circ}\text{K})$	$\frac{[\text{O}_2]}{\times 10^{+5}}$ moles/l	$\frac{[\text{C}_2\text{H}_2]}{\times 10^{+5}}$ moles/l	$\frac{[\text{M}]}{\times 10^{+3}}$ moles/l	$t_i(\mu\text{sec})$	$t_{\text{calc.}}(\mu\text{sec})$	Method
1776	5.22	0.87	1.679	71	65	Total Ioniz., TOF Reflected; in Ne.
1776	5.19	0.87	1.670	76	65	"
1812	5.53	3.68	1.750	49	56	"
1860	2.54	1.69	1.650	89	106	"
1902	5.37	0.90	1.727	42	46	"
1440	4.92	3.28	1.557	364	213	Total Ioniz., TOF Reflected; in Kr.
1452	5.02	3.35	1.589	332	199	"
1474	4.94	3.30	1.563	229	189	"
1496	5.03	3.36	1.593	210	169	"
1519	5.15	3.44	1.632	159	151	"
1543	5.04	3.36	1.595	181	141	"
1562	5.29	3.53	1.674	175	125	"
1575	5.25	3.50	1.661	176	120	"
1600	5.31	3.54	1.680	131	111	"
1717	5.47	3.65	1.730	77	74	"
1790	5.63	3.75	1.780	62	58	"
*1650	3.22	3.21	1.81	266	152	Total Ioniz., Langmuir Probe; Incident; in Ar
*1790	3.29	1.02	1.85	181	99	"
*1800	1.76	1.76	1.87	276	180	"
*2115	1.85	0.57	1.94	119	86	"
*2190	1.85	1.85	1.95	73	73	"

TABLE 2 (Page 3)

INDUCTION PERIODS

<u>T(°K)</u>	<u>[O₂] x 10⁺⁵ moles/l</u>	<u>[C₂H₂] x 10⁺⁵ moles/l</u>	<u>[M] x 10⁺³ moles/l</u>	<u>t_i(μsec)</u>	<u>t_icalc.(μsec)</u>	<u>Method</u>
*1377	6.37	19.13	1.869	176	222	Total Ioniz., TOF, Reflected; in Ne.
*1533	6.48	19.45	1.900	106	114	"
*1621	6.65	19.97	1.929	137	81	"
*1648	7.00	21.00	2.052	121	72	"
*1720	7.66	22.98	2.245	84	52	"
*1766	7.29	21.87	2.138	51	49	"
*1798	7.54	22.62	2.212	40	43	"
*1840	7.66	22.98	2.245	34	38	"
*1840	7.47	22.41	2.190	16.5	39	"
*1936	7.75	23.25	2.274	15.5	30	"
*1973	8.11	24.33	2.380	7.5	26	"
*1997	7.87	23.61	2.307	1.5	25	"

(i) Least squares fit to the data:

$$\text{Log}_{10}(t_i[\text{O}_2]) = -(10.56 \pm 0.09) + \frac{(17,060 \pm 1120)}{4.58 T} \quad (\text{in sec., mole/liter units})$$

(ii) t_i calc. was calculated from the equation given in reference (10);

$$\text{Log}_{10}(t_i[\text{O}_2]) = -(10.57 \pm 0.05) + \frac{(17,100 \pm 300)}{4.58 T} \quad (\text{in sec., mole/liter units})$$

*These points were not included in the least squares calculation.

TABLE 3

TIME CONSTANTS FROM CH* LUMINESCENCE AND TOTAL IONIZATION

T(°K)	$\frac{[O_2]}{x 10^{+5}}$ moles/l	$\frac{[C_2H_2]}{x 10^{+5}}$ moles/l	$\frac{[M]}{x 10^{+3}}$ moles/l	$\tau(\mu\text{sec})$	$\tau_{\text{calc.}}(\mu\text{sec})$	Method
1272	8.91	5.94	2.818	34.6	32.3	Total Ioniz., TOF Reflected; in Ne.
1302	9.29	6.20	2.940	50.2	25.8	"
1308	4.72	3.19	1.491	27.8	50.8	"
1344	4.90	3.27	1.552	43.1	40.8	"
1409	9.79	6.52	3.100	27.7	15.1	"
1409	9.67	6.45	3.059	23.9	15.3	"
*1431	4.89	3.26	1.547	8.7	27.6	"
1450	5.06	3.38	1.602	27.5	24.8	"
1500	2.26	1.51	1.468	53.0	45.4	"
1539	5.21	3.48	1.649	16.3	17.1	"
1558	10.42	6.95	3.680	14.3	8.0	"
1627	5.31	3.54	1.680	13.2	12.5	"
1634	2.37	1.58	1.540	15.6	26.6	"
1692	2.39	1.59	1.552	29.1	22.0	"
1700	5.60	3.73	1.772	12.3	9.2	"
1729	5.70	3.80	1.803	10.8	8.4	"
1749	2.38	1.59	1.547	19.4	19.2	"
1764	5.73	3.82	1.815	9.7	7.6	"
1771	5.64	3.76	1.785	12.1	7.4	"
1812	5.53	3.68	1.750	7.3	6.9	"
1860	2.54	1.69	1.650	18.9	13.4	"
2114	2.70	1.80	1.757	6.3	7.2	"
2196	6.06	4.05	1.918	4.5	2.7	"

(i) Least squares fit to the data:

$$\log_{10}(\tau[O_2]) = -(11.38 \pm 0.12) + \frac{(17,000 \pm 1,610)}{4.58 T} \quad \left(\begin{array}{l} \text{in sec.,} \\ \text{mole/liter units} \end{array} \right)$$

TABLE 3 (Page 2)

TIME CONSTANTS FROM CH* LUMINESCENCE AND TOTAL IONIZATION

T(°K)	$\frac{[O_2]}{x 10^{+5}}$ moles/l	$\frac{[C_2H_2]}{x 10^{+5}}$ moles/l	$\frac{[M]}{x 10^{+3}}$ moles/l	$\tau(\mu\text{sec})$	$\tau_{\text{calc.}}(\mu\text{sec})$	Method
1409	3.11	0.96	1.76	64.1	47.6	Total Ioniz., Langmuir Probe; Incident; in Ar.
1409	3.11	0.96	1.76	62.1	47.6	"
1615	3.22	0.99	1.81	52.2	21.0	"
1625	3.22	0.99	1.81	36.6	20.5	"
1625	3.22	3.21	1.81	28.2	20.5	"
1800	1.76	1.76	1.87	39.1	22.2	"
1933	3.33	3.32	1.86	15.4	8.5	"
2115	1.85	0.57	1.94	20.1	10.5	"
2190	1.85	1.85	1.95	10.5	9.0	"
1409	3.11	0.96	1.76	64.1	47.6	CH* Luminescence; Incident; in Ar.
1409	3.11	0.96	1.76	71.5	47.6	"
1596	3.22	0.99	1.81	36.6	22.5	"
1625	3.22	3.21	1.81	28.2	20.5	"
1800	1.76	1.76	1.87	36.2	22.2	"
1810	1.77	0.54	1.86	40.6	21.5	"
1933	3.33	3.32	1.86	15.4	8.5	"
2115	1.85	0.57	1.94	19.4	10.5	"
2190	1.85	1.85	1.95	13.4	9.0	"

(ii) Least squares fit to the data:

$$\log_{10}(\tau[O_2]) = -(11.25 \pm 0.08) + \frac{(16,900 \pm 1,340)}{4.58 T} \quad (\text{in sec., mole/liter units})$$

$\tau_{\text{calc.}}$ was calculated from the equation given in reference (10).

*This point was not included in the least squares calculations.

TABLE 4

TIME CONSTANTS FOR CO, H₂O AND CO₂ FORMATIONRuns with 3.75 O₂ + 1.25 C₂H₂ + 95 Kr

<u>T(°K)</u>	<u>[O₂](moles/l)</u>	<u>t(μsec)</u>	<u>CO(mm)*</u>	<u>CO₂(mm)</u>	<u>H₂O(mm)</u>
1700	5.36 x 10 ⁻⁵	250	1.4	0.4	--
		300	2.0	0.8	0.2
		350	2.8	1.2	1.4
		400	4.3	1.2	2.2
		450	5.3	1.4	2.4
		500	4.8	1.5	2.6
1703	4.86 x 10 ⁻⁵	400	1.0	0.3	0.4
		450	1.8	0.6	0.8
		500	2.6	1.4	0.8
		550	4.2	--	1.8
		600	4.3	2.4	2.1
1762	4.72 x 10 ⁻⁵	400	0.8	0.2	--
		450	0.4	0.2	0.2
		500	0.8	0.8	0.8
		550	1.8	0.5	0.7
		600	3.2	1.5	0.8
		650	3.4	2.0	0.8
1786	5.48 x 10 ⁻⁵	200	1.0	0.3	0.5
		250	2.2	1.4	0.7
		300	1.9	1.1	0.9
		350	5.1	1.3	1.4
		400	4.3	1.7	2.4

TABLE 4 (Page 2)

TIME CONSTANTS FOR CO, H₂O AND CO₂ FORMATIONRuns with 3.75 O₂ + 1.25 C₂H₂ + 95 Kr

<u>T(°K)</u>	<u>[O₂](moles/l)</u>	<u>t(μsec)</u>	<u>CO(mm)*</u>	<u>CO₂(mm)</u>	<u>H₂O(mm)</u>
1825	4.98 x 10 ⁻⁵	500	1.2	1.5	0.6
		550	2.2	1.1	1.1
		600	--	1.2	1.4
		650	3.3	1.7	1.6
		700	4.3	3.2	2.2
		750	5.6	2.3	3.4

 $\tau_{\text{O.C.G.M.}}$ (μsec) 172±20 179±26 152±21

*Peak heights in millimeters deflection on the scope face.

TABLE 5

TIME CONSTANTS FOR C_4H_2 AND CO FORMATIONRuns with $1.25 O_2 + 3.75 C_2H_2 + 95 Kr$

<u>T(°K)</u>	<u>[O₂](moles/l)</u>	<u>t(μsec)</u>	<u>C₄H₂(mm)*</u>	<u>CO(mm)</u>
1706	1.67 x 10 ⁻⁵	350	0.5	1.1
		400	0.8	1.2
		450	1.2	1.8
		500	1.3	1.9
		550	1.4	1.4
1710	1.71 x 10 ⁻⁵	350	0.6	1.9
		400	0.7	1.0
		450	0.9	1.3
		500	1.0	1.5
		550	2.0	2.1
1711	1.77 x 10 ⁻⁵	250	0.8	1.6
		300	0.9	0.9
		350	0.5	1.3
		400	0.9	1.7
		450	1.6	3.1
		500	2.3	4.0
		550	2.1	2.5
1717	1.70 x 10 ⁻⁵	600	1.5	2.8
		250	1.4	2.0
		300	0.5	0.9
		350	0.9	2.7
		400	2.1	2.8
		450	1.9	3.2
		500	3.0	4.2
		550	2.4	5.4
		600	2.4	3.8
<u>τ_oC.G.M. (μsec)</u>			244±35	340±67

*Peak heights in millimeters deflection on the scope face.

TABLE 6

TIME CONSTANTS FOR CO AND $C_3H_3^+$

$T(^{\circ}K)$	$[O_2](\text{moles/l})$	$[C_2H_2](\text{moles/l})$	No. of Meas.		CO		$C_3H_3^+$	
			CO	$C_3H_3^+$	$\tau(\mu\text{sec})$	$\tau_0(\mu\text{sec})$	$\tau(\mu\text{sec})$	$\tau_0(\mu\text{sec})$
1206	3.98×10^{-5}	2.66×10^{-5}	11	9	136 ± 22	42 ± 7	81 ± 6	25 ± 2
1370	4.60×10^{-5}	3.06×10^{-5}	8	7	77 ± 12	65 ± 10	47 ± 6	39 ± 5
1383	4.10×10^{-5}	2.74×10^{-5}	9	8	90 ± 37	75 ± 31	45 ± 4	38 ± 4
1410	4.54×10^{-5}	2.96×10^{-5}	7	6	51 ± 4	50 ± 4	34 ± 5	33 ± 5
1477	4.82×10^{-5}	3.20×10^{-5}	5	5	39 ± 5	54 ± 7	26 ± 2	35 ± 3
1526	5.01×10^{-5}	3.34×10^{-5}	5	4	29 ± 2	49 ± 3	16 ± 1	27 ± 2

τ_0 C.G.M. for CO is $57.7 \pm 3.3 \mu\text{sec}$.

τ_0 C.G.M. for $C_3H_3^+$ is $33.7 \pm 1.5 \mu\text{sec}$.

τ calculated from eq. (i) TABLE 3 is $38.6 \mu\text{sec}$. for C.G.M. conditions.

Stated errors are standard deviations in the time constants.

See the text for the exact definition of τ_0 and τ_0 C.G.M. Also see Figure 3 for the C.G.M. plot of the data.

TABLE 7

RATIOS* OF PROBE CURRENT TO CHEMILUMINESCENCE INTENSITY

T(°K)	$\frac{[O_2]}{x 10^{+5}}$ moles/liter	$\frac{[C_2H_2]}{x 10^{+5}}$ moles/liter	$\frac{[Ar]}{x 10^{+3}}$ moles/liter	τ (Probe) μsec.	τ (Photocell) μsec.	Ratio Probe Current ÷ Luminescence
1890	1.17	0.29	7.8	--	5.0	0.05
1890	1.17	0.58	7.8	5.7	6.1	0.25
1845	1.17	1.17	7.8	5.6	4.6	0.15
1900	1.08	1.54	7.2	--	6.9	less than 0.1
2020	1.02	0.25	6.8	5.4	4.6	0.23
2080	1.02	0.51	6.8	4.3	4.3	0.50
2081	1.02	1.02	6.8	3.5	4.0	0.25
2281	0.90	0.22	6.0	3.0	3.9	0.78
2281	0.90	0.45	6.0	3.5	3.3	0.75
2238	0.90	0.90	6.0	3.5	3.5	0.16
2238	0.90	1.29	6.0	3.9	3.9	0.75
* Determined over the exponential parts of the time curves. *** The data tabulated above this point were obtained with a different probe.						
1940**	1.20	0.30	7.8	8.3	8.3	0.5
2000	1.21	0.60	8.0	4.8	4.8	0.3
1876	1.20	1.20	7.8	9.6	9.6	0.22
2197	1.06	0.53	7.1	4.3	--	0.5
2062	1.05	1.05	6.8	6.1	7.8	0.2
2100	1.05	2.35	6.9	5.4	--	<0.2
2300	0.95	0.24	6.0	4.8	6.1	1.06
2197	0.92	0.46	6.0	7.5	8.3	0.35
2238	0.93	0.93	6.0	4.3	5.4	0.27
2238	0.93	2.10	6.0	5.7	--	<0.05

Fig. 1

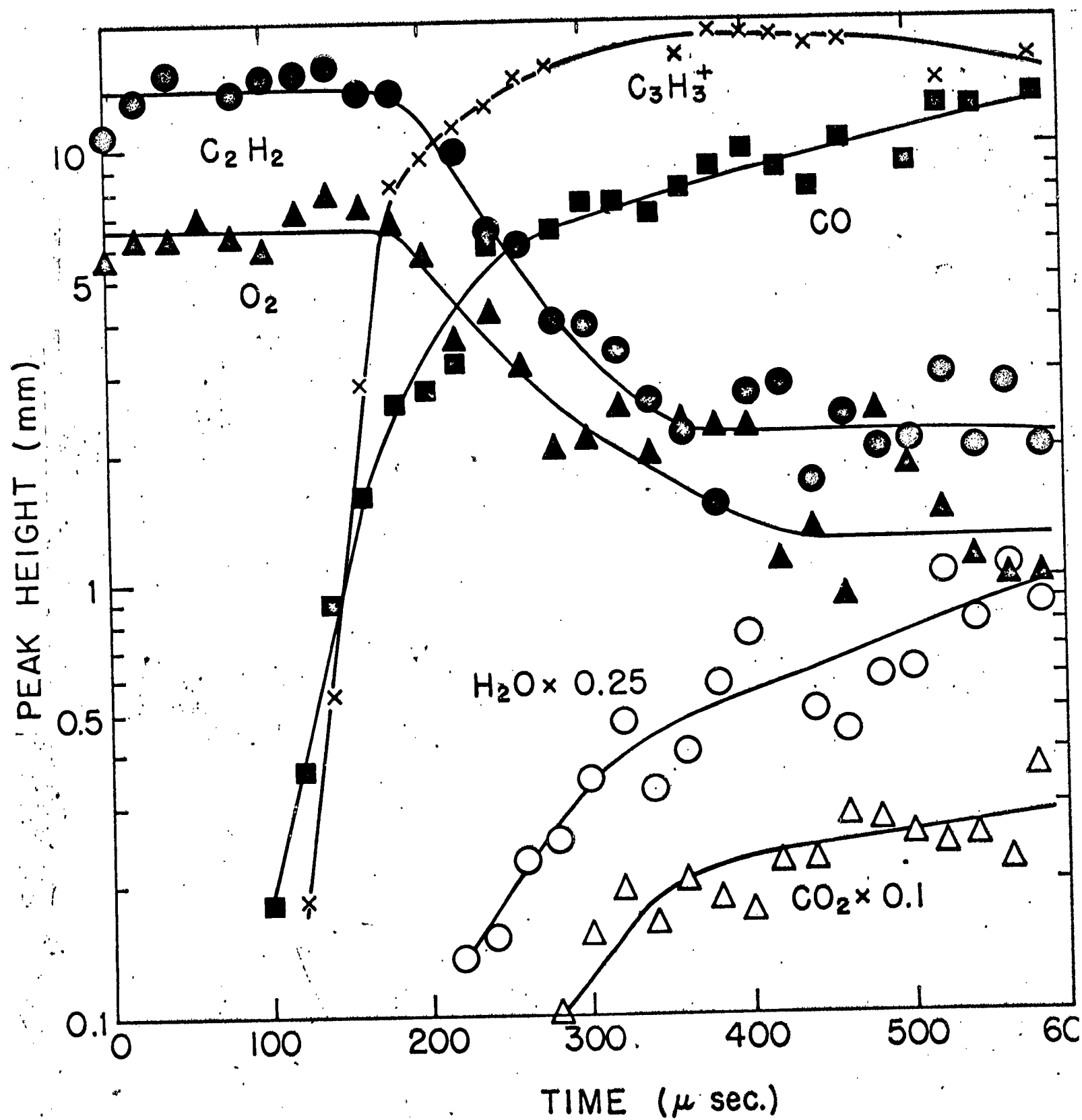
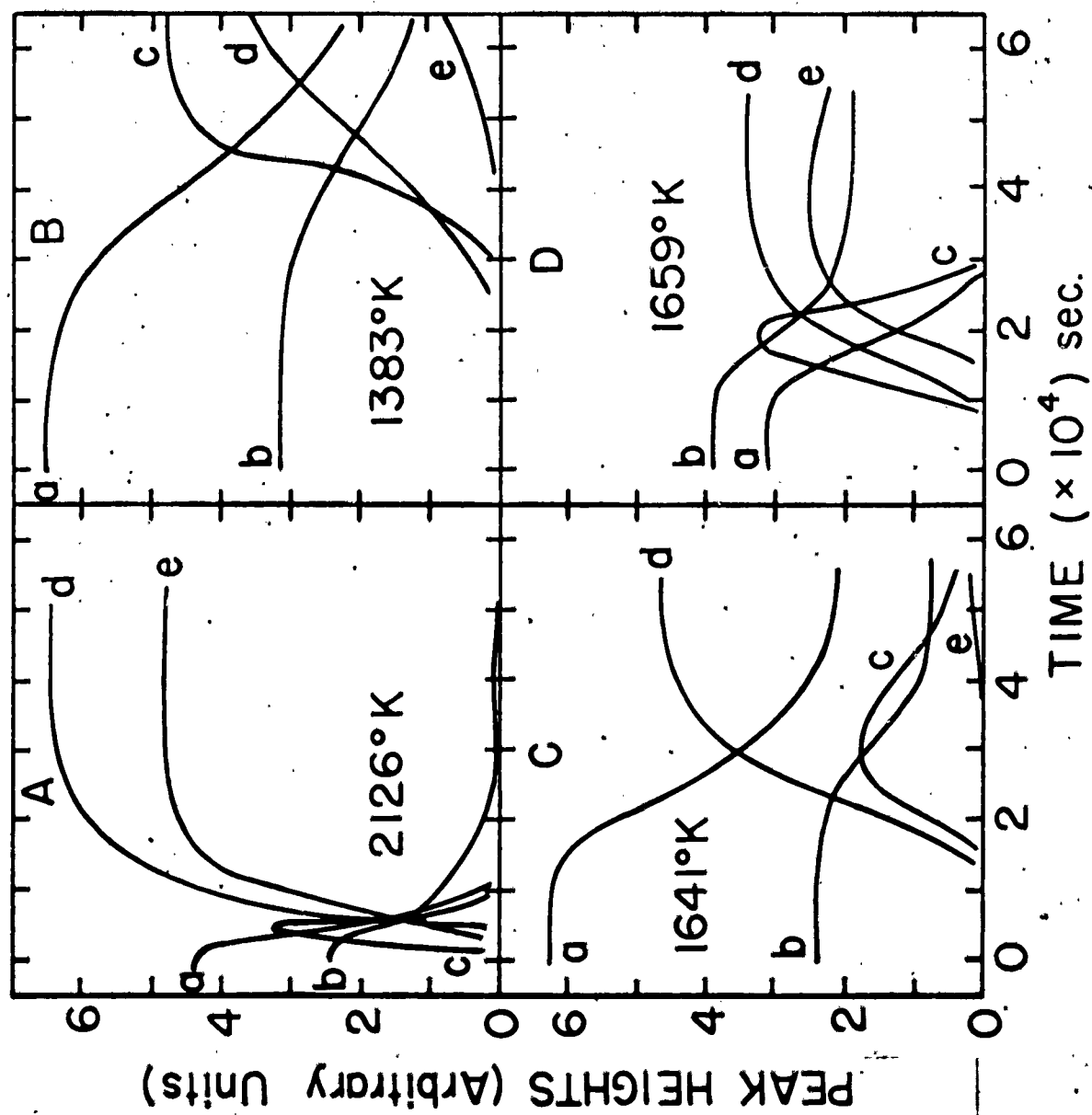


Fig. 2



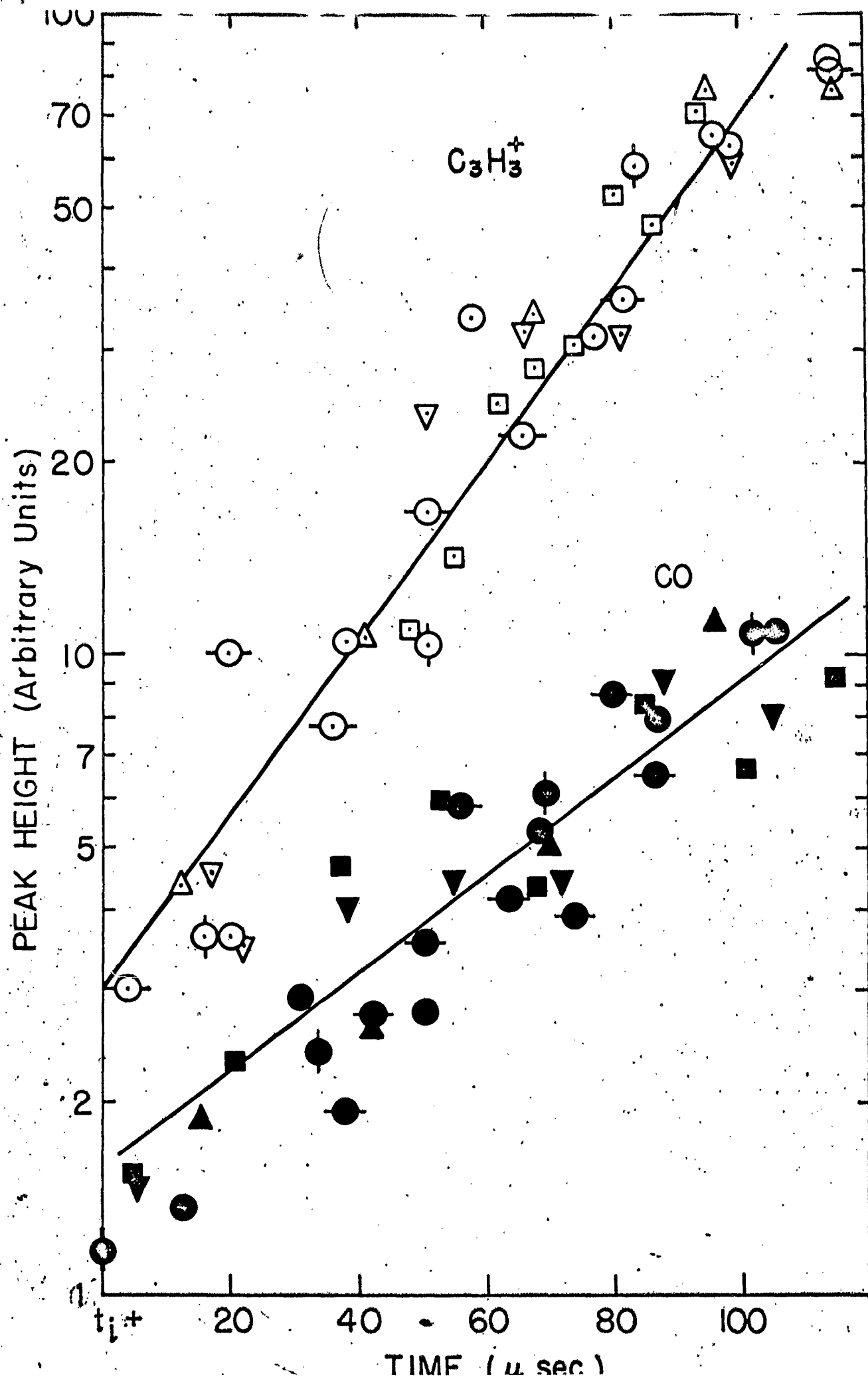


Fig. 3

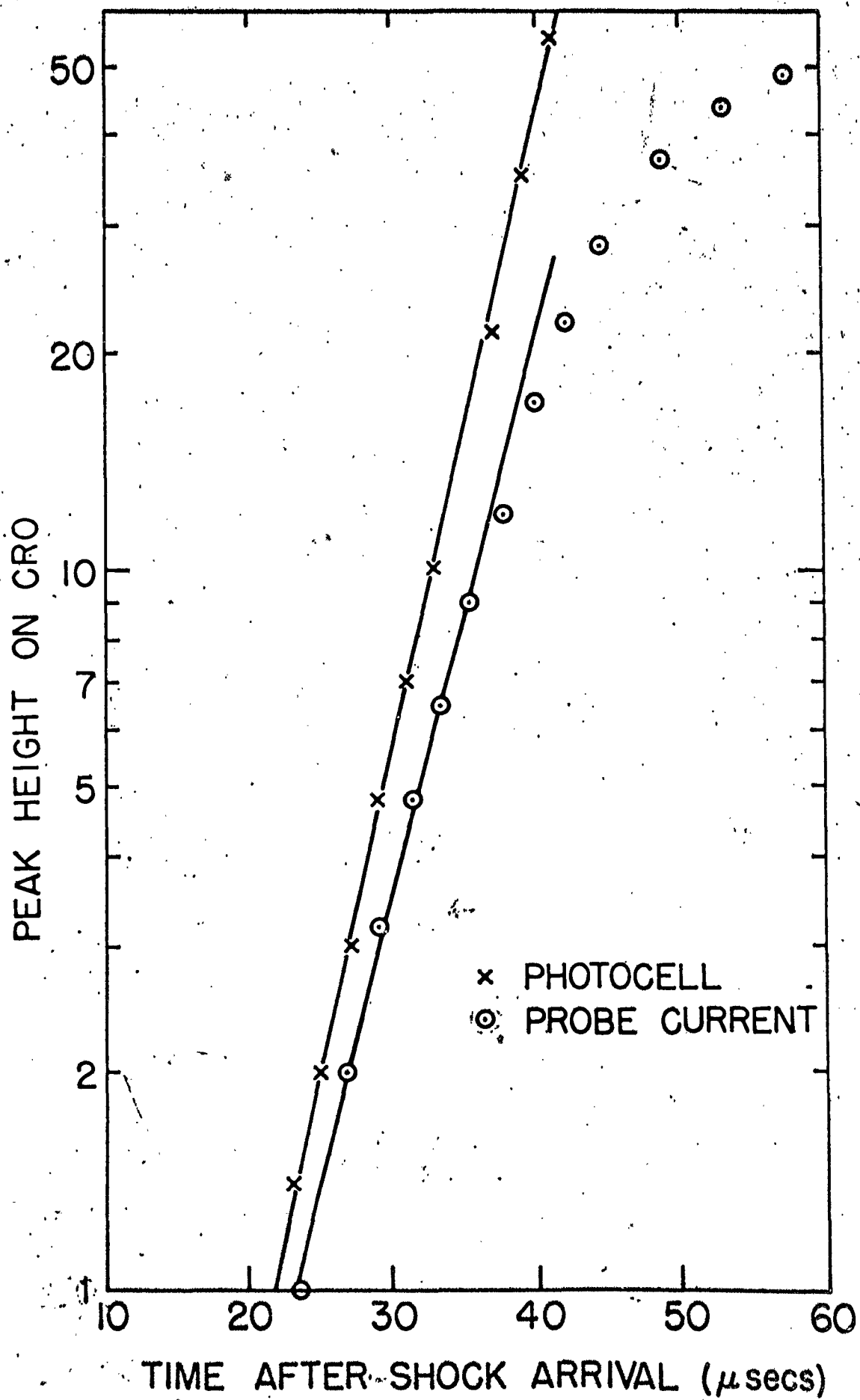


Fig. 4